International Journal of Environmental Sciences
ISSN: 2229-7359
Vol. 11 No. 20s, 2025
https://theaspd.com/index.php

# Spatial Distribution Of Available Manganese In Selected Areas Of Basrah Province Using Geospatial Technologies

**Mohammed J. M. Al-Mayahi[1], Salah M. S. Al-Atab[2], Mohammed A. Abdul Kareem[3]**
[1,2,3]Department of Soil and Water Resources Sciences, College of Agriculture, University of Basrah, Iraq
mohammed.mustafa@uobasrah.edu.iq,salah.sultan@uobasrah.edu.iq,Mohammed.abdulkareem@uobasrah.edu.iq

***Abstract***
*To evaluate and map the spatial distribution of available manganese in agricultural soils of Basrah Province in southern Iraq using geospatial technologies, two regions were selected in the northern and southern of Basrah, with respective areas of 34,561.50 and 4,086.58 hectares respectively. A total of 36 representative samples were collected from each study region, synchronized with the satellite imagery acquisition of Landsat 8 for October 2023. Laboratory analyses were performed, and the correlation between available manganese and selected soil properties was assessed. In the northern region, available manganese content fell within the medium range across the entire area (100%), ranging from 8.93 to 15.80 mg kg⁻¹. In the southern region, 63% of the area showed manganese deficiency, 30% had low levels, and only 7% exhibited medium levels ranging from 0.12 to 10.83 mg kg$^{-1}$. These findings indicated that the studied soils require and respond well to manganese fertilization. A significant negative correlation (r = -0.354) was observed between available manganese and total carbonate content in the southern region.*
***Keywords**: Micronutrients, Available Manganese, Geospatial Technologies, Spatial Distribution.*

## 1. INTRODUCTION

Micronutrients are essential elements needed by plants in small quantities for growth and development. These nutrients include iron, zinc, copper, manganese, boron, molybdenum, and chloride. However, excessive use and accumulation of these elements in soil may lead to environmental pollution, affecting soil and water quality as well as toxicity for plants. Therefore, it is preferable to add the required quantities based on soil analysis and crop requirements to minimize their harmful environmental effects. Additionally, modern soil management techniques such as crop rotation and the use of organic fertilizers help maintain micronutrient balance. Micronutrient deficiencies are widespread due to soil characteristics such as high pH, low organic matter, salt stress, extended drought, and high bicarbonate levels in irrigation water, along with unbalanced fertilizer usage (Syed et al., 2023; Malakouti, 2008). Despite high concentrations, only a small portion is plant-available, and deficiencies may severely affect crop productivity. Different crops respond differently to micronutrients.

Manganese plays a vital role in oxygen production and photosynthesis as it is involved in critical compounds, nitrate reduction, and chlorophyll formation. Tümer et al. (2022) noted that manganese acts as a co-factor for around 35 enzymes and is involved in ATP synthesis, fatty acid and protein biosynthesis, chlorophyll, amino acids, and proteins. Excess manganese leads to oxidative stress by altering enzyme activity and uptake of elements like calcium, magnesium, iron, and phosphorus, ultimately reducing plant growth and causing leaf chlorosis and necrosis. Gupta et al. (2008) described manganese deficiency symptoms as chlorosis on upper to middle leaves and delayed flowering, with leaf color turning gradually from green to yellow. For wheat, the requirement is about 0.02% of the dry weight, while concentrations above 400 ppm cause toxicity (Solanki, 2021).

Remote sensing technologies are asset of that use airborne or space-based sensors, for collecting objective and immediate information about earth's surface or atmosphere. Remote sensing relies on data and providing a database that can be used in the future to study any phenomenon and compare over repeated time periods for a wide area outside researcher controlling and classify the lands (Kumar et al.,2019). Fertility survey is a priority in such studies and using this technique, and preparing spatial distribution maps for fertility assessment of nutrients. Therefore, this study aims to determine the available manganese content and its spatial distribution using remote sensing technologies to save time and reduce costs.

## 2. MATERIALS AND METHODS

### 2.1 Study Area

The study was conducted in two regions: northern and southern parts of Basrah province, Iraq. The first region was in Safwan district, located in the southern part of Iraq. This region lies between longitudes 47°31′ and 47°53′ E, and latitudes 29°59′ and 30°16′ N. It is bordered by Dhi Qar province at the north, the Gulf at the southwest, and Al-Zubair district at the east with a total area of 4,086.58 hectares. The second region is situated between longitudes 47°14′ and 47°42′ E, and latitudes 30°54′ and 31°11′ N. It is bordered by Maysan province at the north, Al-Hartha district at the south, Al-Zubair district at the west, and Iran at the east with a total area 34,561.50 hectares (Figure 1).

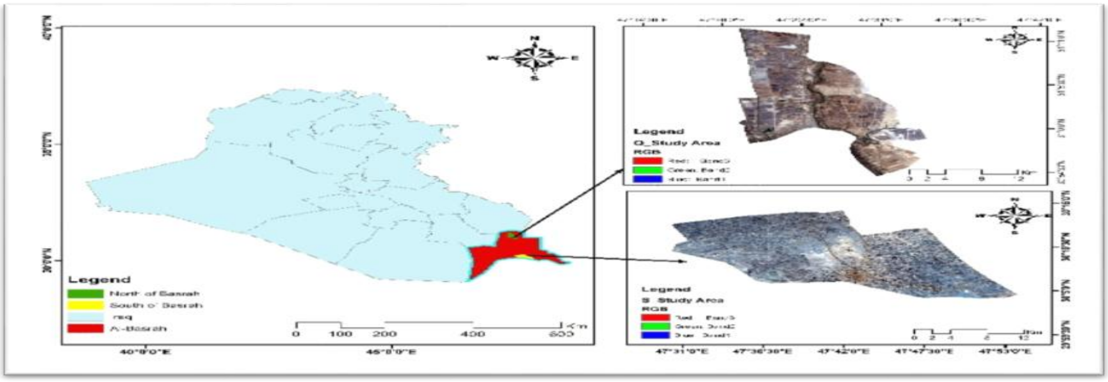


**Figure 1: Location of the study regions**

**2.2 Sample Collection and Laboratory Analysis**

Soil samples were collected from a depth of 0–15 cm, with a total of 36 composite samples randomly taken from each study region in October,2023. All sampling was taken from agricultural lands cultivated with wheat, as shown in Figure 2. Samples of air-dried soil, passed through a 2 mm sieve, were subjected to analysis of pH, electrical conductivity, organic matter content, total carbonates, texture and available content of Mn. Available manganese was measured using Atomic Absorption Spectrophotometry (AAS) after extracting with DTPA-TEA-$CaCl_2$ solution as describe by Norvell and Lindsay (1978). Particle size distribution (text her) was determined using the pipette method (Black et al., 1965). Electrical conductivity (EC) was measured in a 1:1 soil-water extract using conductivity-meter at 25°C (Page et al., 1982). Soil pH was measured in a 1:1 soil-water suspension using pH-meter (Page et al., 1982). Total carbonate minerals were estimated using Jackson’s (1958) method by reacting soil with 1N HCl and titrating the residual acid with 1N NaOH using phenolphthalein as an indicator. Organic carbon was determined by the Walkley–Black method (Page et al., 1982), involving oxidation with potassium dichromate in the presence of sulfuric acid, followed by titration with ammonium ferrous sulfate then Organic matter content was calculated by multiplying the organic carbon percentage by a factor of 1. 724.Corellation coefficient between available Mn amount and different soil characteristics was done using spss program.

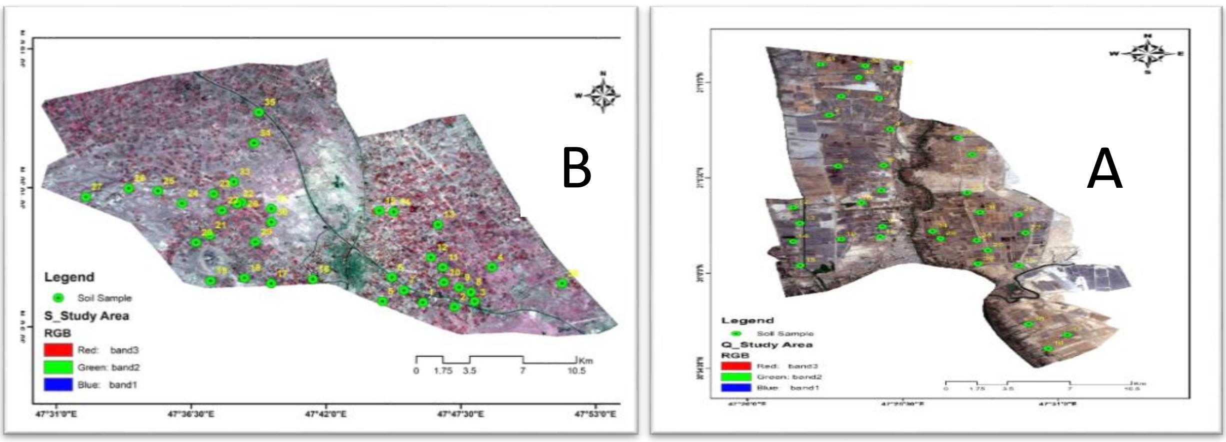


**Figure 2: Study points in the North (A) and South (B) of Basra**

**3.Spatial Distribution of Available Manganese in Soil**

Databases were established for soil unit maps, sampling site locations, and spatial distribution maps of soil properties using the Kriging interpolation method, specifically the Ordinary type with a Spherical model, as illustrated in Figures 4 and 5. This approach was based on the methodology described by

Burroughs and McDonnell (2000). Additionally, the spatial classification of chemical properties followed the Kriging method used for physical soil properties, as outlined by Abdulmanov et al. (2021). ArcGIS 10.4.1 software was utilized for data entry, storage, retrieval, and for building and linking spatial and descriptive databases with other software tools. The outputs were presented in the form of maps, charts, and tables. It is essential to eliminate the atmospheric effects that alter components of electromagnetic radiation as it passes through the atmosphere, particularly when using satellite imagery from multiple dates or for land cover classification. Converting Digital Numbers (DN) to reflectance values is a critical step in this study, as it minimizes the effects of electromagnetic energy absorption and scattering at the time of image acquisition. Landsat 8 satellite images from October 2023, obtained from the U.S. Geological Survey (USGS), were used to improve the accuracy of land cover classification using the following equations:

**Equation (1):**

$L\lambda = ML \times Qcal + AL$

Where:

$L\lambda$ = Spectral radiance (W/(m²·µm))

ML = Radiance multiplicative scaling factor (RADIANCE_MULT_BAND_n from metadata)

AL = Radiance additive scaling factor (RADIANCE_ADD_BAND_n from metadata)

Qcal = Level 1 pixel value in DN

**Equation (2):**

$\rho\lambda' = M\rho \times Qcal + A\rho$

Where:

$\rho\lambda'$ = Top-of-atmosphere planetary reflectance without sun angle correction (unitless)

$M\rho$ = Reflectance multiplicative scaling factor (REFLECTANCE_MULT_BAND_n from metadata)

$A\rho$ = Reflectance additive scaling factor (REFLECTANCE_ADD_BAND_n from metadata)

Qcal = Level 1 pixel value in DN

Note: $\rho\lambda'$ does not represent true top-of-atmosphere reflectance, as it lacks sun angle correction. This correction was intentionally excluded from Level 1 scaling based on user requirements—some users are satisfied with the sun elevation angle from the image metadata, while others prefer to compute their own sun elevation angle per pixel. Once the sun elevation angle is determined, the true top-of-atmosphere reflectance is calculated as:

**Equation (3):**

$\rho\lambda = \rho\lambda' / \sin(\theta)$

Where:

$\rho\lambda$ = Top-of-atmosphere reflectance (unitless)

$\theta$ = Sun elevation angle (from metadata or calculated)

The sun elevation angle is given in degrees, and the date is formatted as "YYDDDHH", where the three "D" digits represent the day of the year. Note that the sine function in ArcMap requires the angle in radians rather than degrees. Convert degrees to radians using:

**Equation (4):**

$\text{Radians} = (\text{degrees} \times \pi) / 180$

## 4. RESULTS AND DISCUSSION

Table 2 and Figure 3 illustrated the available manganese content in northern Basra. Based on the classification by Das et al. (2020) table (1) the available manganese content in the area (100%) was within the medium range, ranging from 8.93 to 15.80 $mg \cdot kg^{-1}$, despite high levels of total carbonates, alkaline pH, and soil salinity, particularly in the central and southern parts of the region. The maintained medium manganese availability may have attributed to the fine-textured of the soil in this region, which reduces manganese losses through adsorption on soil colloidal surfaces. Singh et al. (2014) observed increased manganese availability with higher clay content due to increased cation exchange capacity and availability of exchange sites. Similarly, Salih and Khalil (2013) found that higher clay and silt contents in the soil enhance manganese retention and availability. Organic matter content in this region may also contribute to increased manganese availability, as its relatively uniform distribution allows for the release of manganese-chelating substances during decomposition, such as aliphatic acids, siderophores, phenolic, and Humic acids (Stevenson, 1991). These results suggest that the effect of clay content and organic matter on manganese availability outweighs the negative effects of carbonates, pH, and salinity's.

Additionally, farmers' field practices, including fertilization and irrigation management, may further influence manganese availability. For instance, water quantity affects redox potential (Mn becomes available at Pe + pH < 20.61). Moreover, Mn interactions with other nutrients can alter availability—ammonium and ferrous fertilizers and chloride presence in soil enhance manganese availability, while high phosphorus and magnesium levels reduce it (Prasad and Power, 1997). Based on the manganese content in this region, application of 3–5 pounds per acre (3.39-5.65 kg $ha^{-1}$) of manganese fertilizer is sufficient to meet crop requirements (Jones, 2001; table 5). Table 2 and Figure 4 present the available manganese contents and spatial distribution in southern Basra region. According to Das et al. (2020), 63% of the area (27,937.73 hectares) was classified as manganese-deficient, 30% (13,014.07 hectares) as low in manganese, and only 7% (3,125.02 hectares) as having medium manganese content. These findings indicated that the soils in this region require and are responsive to manganese fertilization. Deficiency was concentrated in the western and parts of the eastern sections of this region of this region, while the highest values were found in the southeastern area (fig.4). The western part showed higher total carbonate levels (160–240 $g\cdot kg^{-1}$) compared to the southeastern part (150–184 $g\cdot kg^{-1}$). A significant negative correlation (r = -0.354) was observed between available manganese and total carbonates (Table 4). Calcium carbonate raises soil pH and reduces manganese availability by promoting oxidation and hydroxide complex formation. The correlation coefficient between carbonate content and available manganese was -0.447 (Kumar and Babel, 2011). Misra and Mishra (1969) and Zhu et al. (2001) also found that calcium carbonate reduces manganese availability by increasing pH, reducing $Mn^{2+}$ concentration, and promoting adsorption or precipitation as manganese carbonate. According to the classification, soils in southern Basra require manganese fertilizer applications at rates of 5–7 pounds per acre (5.65-7.91 kg $ha^{-1}$) for the deficient and low classes, and 3–5 pounds per acre (3.39-5.65 kg $ha^{-1}$) for the medium class. However, the appropriate application rate should consider soil type and crop sensitivity to manganese.

**Table 1: Classification of micronutrients (mg kg-1)**

| NO. | Element | Loss | Few | Medium | High |
|---|---|---|---|---|---|
| 1 | Iron | > 4.5 | 4.5-9.0 | 9.0-27.0 | < 27.0 |
| 2 | Zinc | > 0.6 | 0.6-1.2 | 1.2-2.4 | < 2.4 |
| 3 | Manganese | > 2.0 | 2.0-4.0 | 4.0-16.0 | < 16.0 |
| 4 | Copper | > 0.2 | 0.2-0.4 | 0.4-1.2 | < 1.2 |

**Table 2: Available Manganese in (mg $kg^{-1}$) the Northern Basrah Region**

| Site | Mn | Site | Mn | Site | Mn |
|---|---|---|---|---|---|
| 1 | 15.32 | 13 | 15.04 | 25 | 13.53 |
| 2 | 15.03 | 14 | 12.96 | 26 | 14.51 |
| 3 | 15.43 | 15 | 13.90 | 27 | 8.93 |
| 4 | 15.46 | 16 | 15.51 | 28 | 14.92 |
| 5 | 15.09 | 17 | 15.46 | 29 | 13.66 |
| 6 | 15.08 | 18 | 15.80 | 30 | 11.64 |
| 7 | 12.01 | 19 | 12.65 | 31 | 13.89 |
| 8 | 12.78 | 20 | 14.08 | 32 | 14.76 |
| 9 | 12.86 | 21 | 9.75 | 33 | 13.95 |
| 10 | 14.93 | 22 | 14.62 | 34 | 9.95 |
| 11 | 14.15 | 23 | 14.45 | 35 | 12.93 |
| 12 | 15.15 | 24 | 15.09 | 36 | 14.36 |

**Table 3. Available Manganese in the Southern Basra Region**

| Site | Mn | Site | Mn | Site | Mn |
|---|---|---|---|---|---|
| 1 | 9.80 | 13 | 1.64 | 25 | 0.22 |
| 2 | 10.83 | 14 | 4.69 | 26 | 0.32 |
| 3 | 7.17 | 15 | 3.94 | 27 | 0.28 |
| 4 | 11.39 | 16 | 1.76 | 28 | 0.33 |
| 5 | 6.29 | 17 | 1.93 | 29 | 0.12 |
| 6 | 6.03 | 18 | 1.97 | 30 | 0.25 |

| | | | | | |
|---|---|---|---|---|---|
| 7 | 8.15 | 19 | 4.21 | 31 | 0.13 |
| 8 | 4.22 | 20 | 1.93 | 32 | 0.17 |
| 9 | 3.57 | 21 | 0.22 | 33 | 0.09 |
| 10 | 5.71 | 22 | 1.10 | 34 | 0.14 |
| 11 | 6.31 | 23 | 0.74 | 35 | 0.10 |
| 12 | 3.03 | 24 | 0.37 | 36 | 0.30 |

**Table 4. Correlation Coefficient Between Available Manganese and Soil Properties in the Northern and Southern Basra Region**

| Parameter | pH | EC | O.M | $CaCO_3$ | Texture |
|---|---|---|---|---|---|
| Northern | -0.068n.s | -0.432** | 0.064n.s | -0.328n.s | 0.170n.s |
| Southern | -0.216n.s | -0.041n.s | 0.034n.s | -0.354* | 0.167n.s |

**Table 5: Concentration of trace elements in soil (mg kg-1)**

| NO. | Element | Very low | Low | Medium | High | Very high |
|---|---|---|---|---|---|---|
| 1 | Iron | 0-5 | 5-10 | 11-16 | 17-25 | < 25 |
| 2 | Zinc | 0-4 | 4-8 | 9-12 | 13-30 | <30 |
| 3 | Manganese | > 0.5 | 0.5-1 | 1.1-3 | 3.1-6 | <6 |
| 4 | Copper | > 0.3 | 0.3-0.8 | 0.9-1.2 | 1.3-2.5 | <2.5 |
| 5 | Boron | > 0.4 | 0.4-0.7 | 0.8-1.2 | 2.0-1.3 | <2.0 |

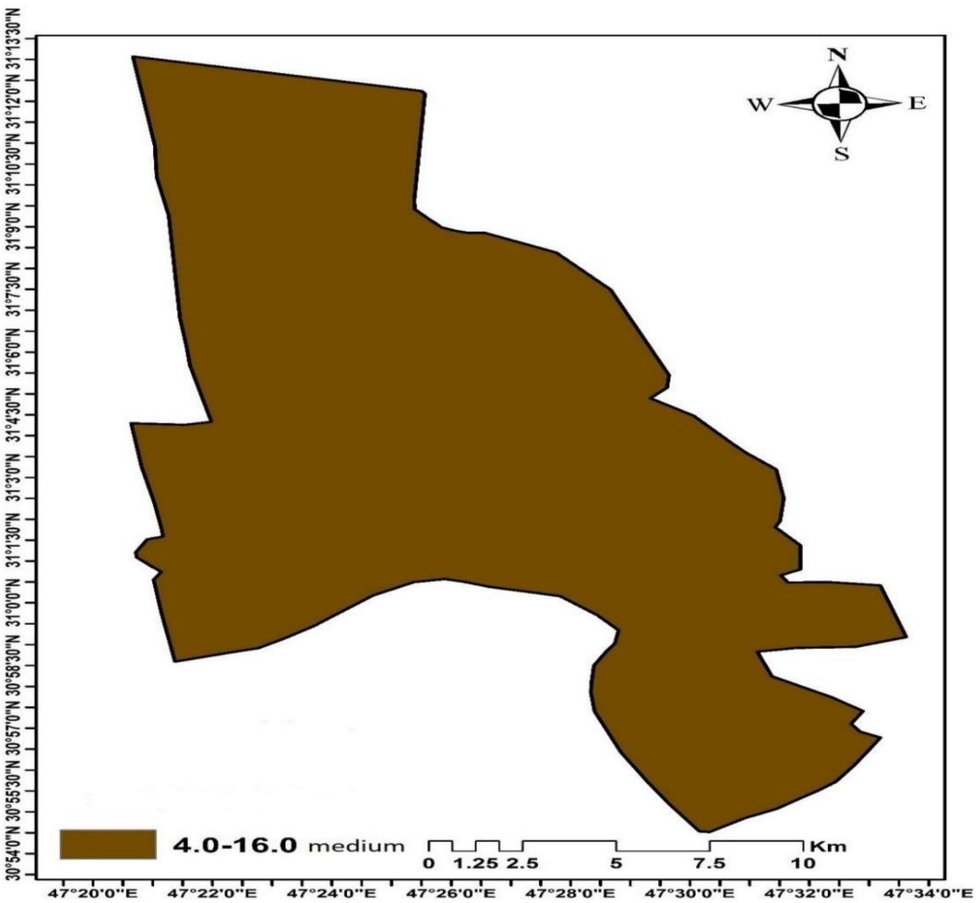


**Figure 3: Spatial distribution of available manganese in northern Basrah region**

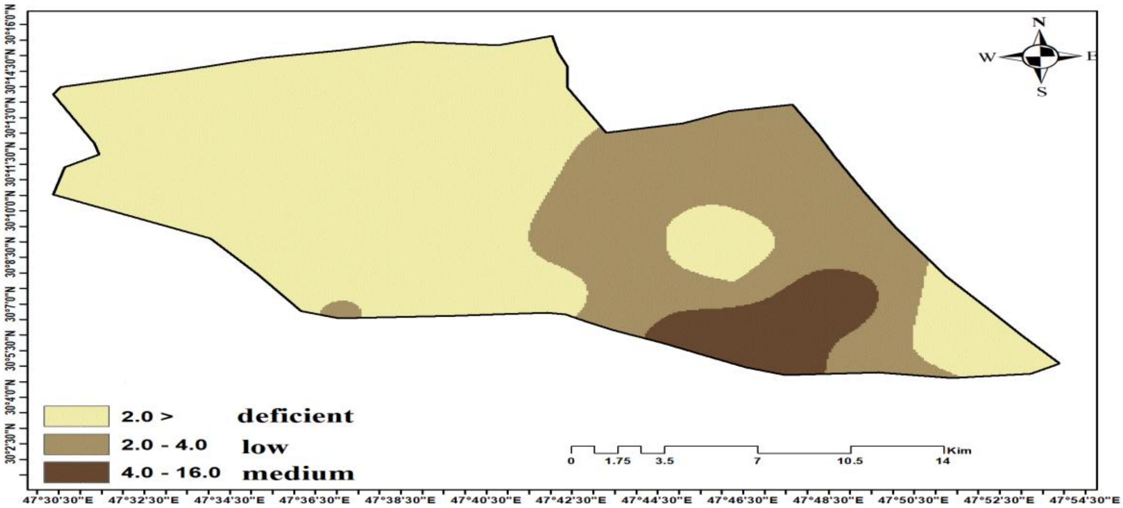


**Figure 4: Spatial distribution of available manganese in southern Basrah region**

## 3. Spectral Reflectance

The spectral reflectance derived from Landsat-8 imagery was analyzed for the study area in southern Basra. As shown in Figure 5, the spectral reflectance of the surface horizon at the sampled points exhibited low values in Band 2, ranging between -0.0742 and -0.0696. Similarly, Band 3 showed low reflectance values ranging from -0.0744 to -0.0677, and Band 8 followed the same trend with values between -0.0744 and -0.0675. Band 6 exhibited slightly lower reflectance values, ranging from -0.0497 to -0.0323. In contrast, Band 7 showed higher reflectance values than the previous bands, ranging from 0.0559 to 0.1179. Band 5 showed values between 0.1303 and 0.1678. The highest reflectance was observed in Band 4, with values ranging from 0.2221 to 0.2895. Similarly, the spectral reflectance from Landsat-8 was analyzed for the study area in northern Basra. As presented in Figure 6, the surface horizon at the study points also showed low reflectance values in Band 2, ranging from -0.0767 to -0.0681. Band 3 ranged from -0.0788 to -0.0734, and Band 8 followed a similar pattern with values from -0.0797 to -0.0709. Band 6 ranged between -0.0863 and -0.0372. Band 7 had relatively higher reflectance values, ranging from 0.0313 to 0.0818. Reflectance in Band 5 ranged from 0.0759 to 0.1299, while the highest reflectance was recorded in Band 4, ranging from 0.1555 to 0.2388.

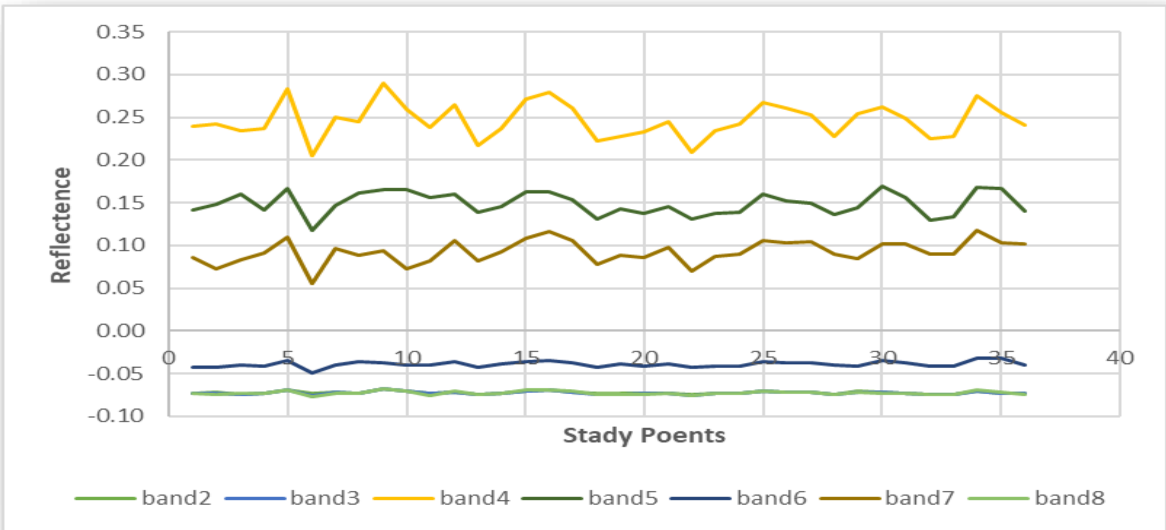


**Figure (5): Spectral Reflectance of Sampling Points in the Southern Basra Region**

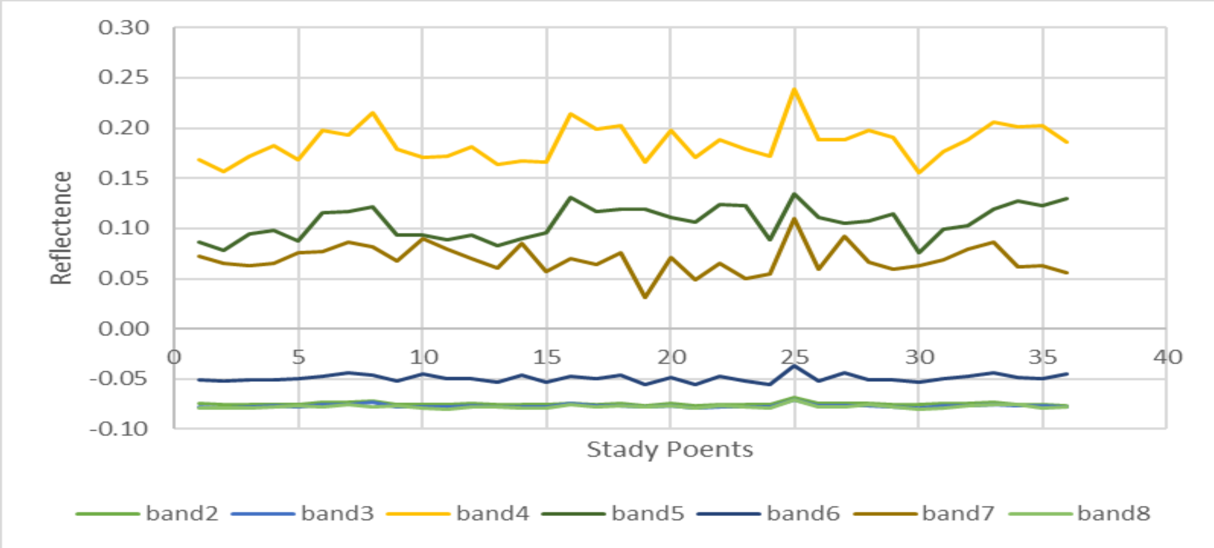


**Figure (6): Spectral Reflectance of Sampling Points in the Northern Basra Region**

As is well known, spectral reflectance represents the ratio of radiation reflected from a surface to the incident radiation upon it at a specific wavelength, with values ranging from 0 to 1. However, negative values may appear in some bands due to numerical effects and correctional processing. Band 2, with a wavelength of 0.45–0.51 µm, corresponds to the blue spectral region and is highly sensitive to scattering. Band 3, with a wavelength of 0.52–0.60 µm, represents the green spectral region, part of which is reflected by vegetation. Band 4, ranging from 0.63–0.68 µm, represents the red spectral region, which is strongly absorbed by chlorophyll. Band 5, at 0.85–0.88 µm, lies in the near-infrared region and exhibits strong reflectance from healthy vegetation. Band 6, at 1.57–1.65 µm, lies in the shortwave infrared region and is characterized by high water absorption. Band 7, with a wavelength of 2.11–2.29 µm, lies in the mid-infrared region and is sensitive to soil dryness. Band 8, at 0.50–0.68 µm, spans a broad spectral range and is used for wide-range spectral integration. Thus, Bands 2, 3, and 8, which lie in the short-wavelength regions (blue and green) and are sensitive to the entire visible spectrum, are significantly influenced by atmospheric scattering. Band 6 falls within a range that exhibits strong water absorption, either from atmospheric moisture or the surface itself, resulting in a marked decrease in reflected radiation, which may yield negative values when converted to surface reflectance. Band 8, sensitive to the full visible spectrum, is designed to capture broad-spectrum light, especially in areas with low radiance. Band 4 typically shows moderate reflectance due to chlorophyll absorption but is less affected by scattering compared to the blue and green bands. Band 5 exhibits high reflectance in healthy vegetation, while Band 7, being less sensitive to moisture and more responsive to soil content, typically produces higher reflectance values. In general, bands with negative values are more affected by atmospheric interference, while bands with positive values indicate stronger surface-reflected radiation or reduced atmospheric noise. Furthermore, increased organic content and soil moisture contribute to higher absorption of incoming radiation and lower reflectance values. This is attributed to the timing of satellite image acquisition, which coincided with land preparation and irrigation activities for leveling and calibration purposes prior to seed sowing (Al-Daraji et al., 2024).

## 4.CONCLUSIONS

1. Available Mn Content in North region was higher (medium class) than that of South region (More than 90% of samples were deficient and low classes).
2. Available Mn content was highly correlated with soil texture and organic matter content that pH, total carbonates and EC.
3. Spatial variability in available manganese was evident between northern and southern Basra, which can be attributed to differences in the studied soil properties.
4. Spectral reflectance showed negative values due to a decline caused by high soil moisture at the time of image acquisition, as the land was being irrigated in preparation for cultivation.

5. Most soils in the study area require the addition of manganese through fertilization. The application should be guided by soil type and crop sensitivity to manganese to achieve optimal productivity and maintain food security.

6. **REFERENCES**

7. **Abdulmanov, R.; Miftakhov, I.; Ishbulatov, M.; Galeev, E., and Shafeeva, E. (2021).** Comparison of the effectiveness of GIS-based interpolation methods for estimating the spatial distribution of agrochemical soil properties. Environmental Technology & Innovation, 24, 101970.https://doi.org/10.1016/j.eti.2021.101970.

8. **Al-Daraji, F.K., Ndewi, D.R., Al-Shammari, H.M. (2024)**. Modeling and Analysis of Land Surface Temperature Variations in Basrah Governorate, Iraq, Using Remote Sensing Data and Geomatics Techniques. In: Obaid, A.J., Al-Heety, E.A., Radwan, N., Polkowski, Z. (eds) Advanced Studies on Environmental Sustainability. ICES 2023. Springer Proceedings in Earth and Environmental Sciences. Springer, Cham. **https://doi.org/10.1007/978-3-031-57054-4_7**

9. **Black, C. A.; D. D. Evans; L. L. White; L. E. Ensminger and F. E. Clark (1965).** Method of soil analysis. Part 1. In Agronomy Series (9). Am. Soc. Agrion.

10. **Burroughs, P. A. and McDonnell R. A. (2000).** Principles of Geographic Information Systems. Oxford University Press, New York.

11. **Das, S., Bag, A. G.; Chatterjee, N., Pal, B.; Ghosh, D. and Hazra, G. C. (2020).** Block wise spatial distribution and mapping of cationic micronutrients in soils of Jhargram District of West Bengal. International Journal of Environment and Climate Change, 10(10): 111-122. **http://www.sdiarticle4.com/review-history/61579**

12. **Jackson, M. L. (1958).** Soil Chemical analysis. Prentice Hall, Inc. Englewood Cliffs. J.

13. **Jones, J. B. (2001).** Laboratory guide for conducting soil tests plant analysis. CRC Press. USA.

14. **Kumar, M. and Babel, A. L. (2011)**. Available micronutrient status and their relationship with soil properties of Jhunjhunu Tehsil, District Jhunjhunu, Rajasthan, India. Journal of Agricultural Science, 3(2) p: 97. **10.5539/jas. v3n2p97**

15. **Malakouti, M. J. (2008).** The effect of micronutrients in ensuring efficient use of macronutrients. Turkish Journal of agriculture and Forestry, 32(3): 215-220. **https://journals.tubitak.gov.tr/agriculture/vol32/iss3/7**

16. **Misra, S. G., and Mishra, B. (1969).** Effect of calcium carbonate on availability of manganese in soils. Plant and Soil, 30(2), 290–296. **https://doi.org/10.1007/BF01373697.**

17. **Norvell, W. A. and Lindsay, W. L. (1978).** Reaction DTPA chelates of iron, zinc, copper, and manganese with soils. Soil sci. soc. Amer. Oroc. 36: 778-783.

18. **Page, A. L.; R. H. Miller and D. R. Keeney (1982).** Methods of soil analysis. Part 2. 2nd ed. ASA. Inc. Madison, Wisconsin, U.S.A.

19. **Prasad, R. and power, J.F. (1997)** • Soil fertility management for sub stainable agriculture. Lewis pub. CRC press LLC.USA.

20. **Salih, A. M., and Khalil, M. T. S. (2013).** Effect of (Clay & Silt) Fractions and Carbonate Minerals on Pedogenical Distribution of Manganese Extracted by Different Methods. Mesopotamia Journal of Agriculture, 41(1): 134–144. **https://doi.org/10.33899/magrj.2013.76025.**

21. **Singh, K. B., Dhaliwal, S. S. and Sikka, R. (2014)**. Effect of climate and soil texture on distribution of micronutrients under continuous rice-wheat system. Indian J Fert, 10(7): 54-56.

22. **Solanki, M. (2021).** The Zn as a vital micronutrient in plants. Journal of microbiology, biotechnology and food sciences, 11(3), e4026-e4026. https://doi.org/10.15414/jmbfs.4026

23. **Stevenson, F. J. (1991).** Organic matter-nutrient reactions in soil, in micronutrients in Agriculture, Motived, J. J.; Cox, F.R.; Shuman, L.M. and Welch, R.M. Eds., Soil Sci. Soc. Am., Madison, WI: 145-186.

24. **Syed, S., Kumar, P., Hashmi, M. and Singh, H. (2023).** Dynamics Importance of Micronutrients in Agricultural Soil. Just Agriculture multidiscipllary e-Newsletter. B (8):157-160.https://www.researchgate.net/publication/370653496

25. **Tümer, C., Çavuşoğlu, K., and Yalçin, E. (2022).** Screening the toxicity profile and genotoxicity mechanism of excess manganese confirmed by spectral shift. Scientific Reports, 12(1), 20986. https://doi.org/10.1038/s41598-022-25657-6

26. **Zhu, Z. L.; Chen, D. L. and Li, S. X. (2001).** Effect of calcium carbonate on manganese forms in calcareous soils. Plant Nutrition and Fertilizer Science, 7(3): 313-318.